Records of Natural Products

Open Access
This article is licensed under CC-BY-NC-ND 4.0

www.acgpubs.org

ORIGINAL ARTICLE

In silico biochemical and structure-based evaluation of *Artemisia annua*-derived compounds against key dengue hemorrhagic fever molecular targets

Mubarak A. Alamri[1*] and Mohamed Ahmed Akela[2]

[1]Department of Pharmaceutical Chemistry, College of Pharmacy, Prince Sattam Bin Abdulaziz University, Al-Kharj, 11942, Saudi Arabia
[2]Department of Biology, College of Science and Humanities in Al-Kharj, Prince Sattam bin Abdulaziz University, Al-Kharj, 11942, Saudi Arabia

Cite This: *Rec. Nat. Prod.* 2027, 21(2), e26073985

Read Online

Abstract: Dengue Hemorrhagic Fever (DHF) continues to be a major public health challenge because of its complicated inflammatory mechanism and lack of an antiviral treatment strategy. The current investigation employs a stringent systems biology approach, including network pharmacology, gene expression studies, and molecular modeling, to identify critical genetic targets in DHF and assess the efficacy of compounds derived from *Artemisia annua* (*A. annua*) in treating this condition. Microarray analysis of the GSE18090 and GSE51808 datasets identified differentially expressed genes associated with DHF development. In addition, network pharmacology revealed that artemisinin, luteolin, aurantiamide, and artemisitene can be used to regulate the host inflammatory response by targeting key hub proteins AKT1, HSP90AA1, and ESR1. These proteins play an important role in signaling and stress-related processes in the cell and are often targeted by viruses. The identified interaction was confirmed by molecular docking and a 100-ns MD simulation, which showed a stable complex with high binding affinity. The findings indicated a high binding affinity and structural stability of the compounds within the active sites of their respective targets, with minimal RMSD fluctuations throughout the simulation trajectory. Our results suggest that derivatives of *A. annua* may alleviate DHF-induced hyperinflammation by targeting multiple proteins. Although these computational insights lay a solid groundwork for drug repurposing, further in vitro and in vivo validation is necessary to verify their efficacy and safety profiles.

Keywords: DHF, DENV, *Artemisia annua*, network pharmacology, molecular dynamics simulations, Gene Expression Omnibus

1 Introduction

Dengue is an infectious disease that is spreading quickly, is transmitted by arthropods, and is caused by the dengue virus (DENV) (Yap et al., 2017). It is a single-stranded positive-sense RNA virus from the Flavivirus family and poses a major global health issue that impacts about two-thirds of the world's population (Sinha et al., 2024; Villordo et al., 2015). This virus can lead to a range of disease severities, from mild symptoms to fatal shock syndrome. Although Dengue has a significant global impact, treatment options remain limited, with no specific antiviral medications and few vaccines available. Four distinct serotypes (DENV 1 to 4) of DENV are present, each with its own genetic makeup (Tuiskunen Bäck & Lundkvist, 2013; Phadungsombat et al., 2024).

However, the variants have been classified as DENV-1 to DENV-4, and the reference sequences have been documented as MW288036.1, KM204118.1, MW288040.1, and KJ596664.1, respectively (Salazar et al., 2014). DENV efficiently manipulates host cell functions through diverse biological mechanisms. Flaviviruses (e.g., DENV) exploit host cellular functions to complete their life cycle and affect host RNA metabolism and the immune system. Upon infection of the host, DENV specifically infects and replicates in dendritic cells; however, it also infects macrophages, lymphocytes, and monocytes. Entry of the virus into the host cell occurs via receptor-mediated endocytosis using Fc receptors, glycosaminoglycans (GAGs), the surface molecule CD14, heparan sulfate, and lectin-like receptors, including DC-SIGN (Sinha et al., 2024; Villordo et al., 2015). DENV enters

*Corresponding Author: Mubarak Alamri.
Email: m.alamri@psau.edu.sa
Received: July 21, 2026
Revised: September 07, 2026
Accepted: September 08, 2026
Published: September 28, 2026

Copyright © 2026. Published by ACG Publications.

host cells via clathrin-coated vesicles, interferes with cellular functions, and produces its components (Salazar et al., 2014; Seema & Jain, 2005). Nonstructural proteins of the virus interfere with the immune response, promoting the dissemination of infection. NS3 and NS4a obstruct RIG-I translocation to mitochondria, whereas NS2a and NS4b suppress the activation of TBK1, preventing MAVS pathway signaling and hindering the production of IFN-β. NS2b suppresses immunity by facilitating GAS degradation through autophagy-lysosomal processes, obstructing mitochondrial DNA detection, and proteolytically cleaving STING to prevent the production of interferons (Uno & Ross, 2018). Additionally, interactions between DENV and host genes directly influence cellular pathways, such as NS5-mediated STAT2 (Transcriptional control), NS1-DIDO1 (epigenetic reprogramming), and dysregulation of RNA splicing and translation. Conversely, the host downstream responses to infection include cytokine storm activation, metabolic reprogramming, interferon signaling, and perturbation of stress granules. These responses serve as defense mechanisms and are frequently manipulated by dengue virus (DENV), thereby facilitating immune evasion, enhancing viral replication, and exacerbating disease severity (Chauhan et al., 2024). Although DENV1 is a severe condition, the infection is associated with key host genes, and the mechanisms of molecular pathogenesis and potential activators or inhibitors remain underexplored. Thus, it is crucial to conduct a more precise investigation of key host genes to elucidate the underlying pathogenic mechanism and identify potential therapeutic agents. However, identifying such key host genes and drug candidates from a vast pool of possibilities is quite challenging with conventional wet-lab experiments alone, as these methods are labor-intensive, time-consuming, and expensive. In this context, bioinformatics approaches play a crucial role in accelerating drug discovery (Khetarpal & Khanna, 2016; Screaton et al., 2015; Brady et al., 2012). *Artemisia annua* (*A. annua*), also known as sweet wormwood, sweet annie, sweet sagewort, or annual wormwood (Chinese: qinghao), is an annual herbaceous plant in the Asteraceae family. *A. annua* is native to temperate Asia and naturalized globally (Swamikannu et al., 2024). *A. annua*, a potent antimalarial medicinal plant, has been widely used in traditional practices such as folk medicine, homeopathy, and Ayurveda. According to the literature, Chinese practitioners traditionally used the aqueous extract of the dried herb to treat fever, malaria, dermatological conditions, jaundice, and hemorrhoids (Nofal et al., 2009). The World Health Organization (WHO) recognizes the importance of artemisinin and its chemical derivatives, which have been widely used as frontline antimalarial drugs worldwide (Patočka & Plucar, 2003). Another study reported that *A. annua* exhibits promising antiviral activity in the lab against SARS-CoV-2 and other viruses, primarily through its extracts and bioactive compounds. While preclinical evidence is strong, clinical trials remain limited, with ongoing phase 2 studies for COVID-19 (Nie et al., 2021). *A. annua* is rich in artemisinin and its derivatives, artesunate, artemether, flavonoids like quercetin and rutin, scopoletin, arteannuin B, artemisinic acid, and essential oils such as alpha-pinene and camphor. These compounds contribute to antiviral, anti-inflammatory, and antioxidant effects (Shaer et al., 2025; Baggieri et al., 2023; Nigam et al., 2019). Several studies show that extracts from *Artemisia* species and their active metabolites may inhibit or modulate viral replication, especially against acute respiratory syndrome coronavirus, diarrhea virus, and RNA viruses (Kshirsagar & Rao, 2021; Nigam et al., 2019; Li et al., 2026). Host molecular research is essential for the effective treatment of dengue hemorrhagic fever (DHF), as it helps assess disease severity and progression. Changes in the gene expression profiles of the host genes linked to the severity of DHF have been discovered through comprehensive transcriptomic and proteomic studies, uncovering pathways associated with immune response activation, signal transduction, and interactions between the host and the virus (Devignot et al., 2010; Sun et al., 2013; Choudhury et al., 2024). In addition, some critical bioinformatics methods, including gene expression analysis, protein-protein interaction network analysis, and gene ontology enrichment analysis, have been pivotal in identifying potential key regulators that can serve as treatment targets or biomarkers in DHF (Pestana & Rodrigues, 2026; Josyula et al., 2023).

Although there have been considerable strides in understanding dengue virus infection, the molecular processes underlying severe conditions such as DHF remain incompletely understood, and effective targeted therapies are lacking. Further research is needed to identify host genes of considerable significance in disease development and to determine their potential as treatment targets. In the current paper, we attempt to fill a gap in the literature by using a bioinformatics approach to investigate the potential of metabolites from *A. annua* to combat dengue virus infection, with a particular focus on DHF. The goal of the investigation is to identify and study key genes involved in the development of DHF, elucidate the underlying molecular mechanisms, and consider potential bioactive compounds as therapeutic agents. These findings contribute to the development of novel, cost-effective, and targeted strategies for the management of severe dengue infections.

2 Materials and Methods

2.1 Data Source and Description

To explore DENVI-causing key genes, publicly accessible gene expression profile datasets were downloaded from the National Center for Biotechnology Information (NCBI) Gene Expression Omnibus (GEO) database (Barrett, 2004) with accession numbers GSE18090 (Nascimento et al., 2009) (Platform GPL570) and GSE51808 (Kwissa et al., 2014) (Platform GPL13158). The comprehensive information on the datasets is summarized in Table 1.

2.2 Rationale for Selecting the Two GEO Datasets

To identify host genes associated with DENV infection and disease severity, two publicly available gene-expression datasets, GSE18090 and GSE51808, were selected because they comprise an early acute febrile dengue cohort from

https://doi.org/10.25135/rnp.2607.3985
Rec. Nat. Prod. 2027, 21(2):e26073985

Table 1. Summary of GEO datasets used in this study

GEO accession	Description	Sample groups and numbers
GSE18090	An array-based transcriptome dataset from a Brazilian cohort of early acute febrile dengue infection (DF and DHF) using the Affymetrix U133A/Plus2.0.	ND (normal febrile dengue-free) = 8; DF = 8; DHF = 10.
GSE51808	Whole-blood array dataset: DF and DHF vs. healthy controls.	Healthy controls = 9; DF = 18; DHF = 10.

Note: DF; Dengue fever. DHF; Dengue hemorrhagic fever.

Brazil, including DF, DHF, and non-dengue febrile controls, with DHF samples collected before the onset of plasma leakage, thereby providing an appropriate model for investigating early molecular changes associated with progression to severe disease. GSE51808 was selected as an independent, complementary dataset comprising whole-blood transcriptomic profiles from patients with acute DF and DHF, along with ND (normal febrile dengue-free). The inclusion of these two independent datasets enabled comparison of host transcriptional responses across different cohorts and disease states. It facilitated the identification of reproducible genes associated with DENV infection and disease severity.

2.3 Identification of Disease-Related Targets

To investigate the host differentially expressed genes (hDEGs) between normal and DENV groups, we adopted a statistical approach using LIMMA (Linear Models for Microarray) (Ritchie et al., 2015). By utilizing the web tool GEO2R (Kalyan et al., 2023) that incorporates the package LIMMA to pinpoint hDEGs across both GEO datasets. LIMMA approach employs an empirical Bayesian technique to improve variance estimation, making it more efficient for smaller sample sizes. Analysis of GEO2R relies on the series matrix files provided by the data submitter, which are pre-processed and normalized using platform-specific methods such as robust multi-array average (RMA) normalization. After identifying hDEGs from each dataset, we applied established thresholds ($|\log2\ FC| > 1$, adjusted p-value <0.05).

2.4 Meta-Analysis Using ImaGEO

We performed a meta-analysis of gene expression data using the ImaGEO platform (Integrative Gene Expression Analysis from the GEO database). ImaGEO (Toro-Domínguez et al., 2018) is a web-based tool that implements a robust and comprehensive meta-analysis pipeline to analyze gene expression datasets directly from GEO identifiers. Gene expression datasets associated with the disease condition were retrieved from the GEO database and selected based on predefined inclusion criteria, including sample type, compatibility with the platform (e.g., Illumina, Affymetrix HTA 2.0, Agilent for human samples), and data quality.

2.5 Identify Bioactive Compounds and Potential Molecular Targets of *A. annua*

We extracted bioactive compounds from the Traditional Chinese Medicine Systems Pharmacological (Daina et al., 2019) (TCMSP) database (https://www.tcmsp-e.com/load_intro.php?id= 43) in July 2025. The key ADME properties of the TCMSP database for filtering bioactive compounds we considered were oral bioavailability greater than 30% and a drug-likeness score greater than 0.18. Subsequently, we evaluated Caco-2 permeability, BBB penetration, and Lipinski's Rule of Five, focusing on molecular weight, hydrogen-bond donors, hydrogen-bond acceptors, and lipophilicity (LogP). Compounds that met the recommended Lipinski criteria and exhibited favorable predicted ADME properties were selected for subsequent molecular docking analysis. Compounds with unfavorable physicochemical or ADME characteristics were excluded from further computational analysis.

We screened bioactive compounds using these criteria and shortlisted eight from *A. annua*. The Swiss Target Prediction Database (Daina et al., 2019) (https://www.swisstargetprediction.ch/citing.php) was utilized to select molecular targets associated with selected bioactive compounds.

For each compound, all predicted targets returned by Swiss Target Prediction were included in the subsequent analysis, without applying any probability-score cutoff or additional filtering criterion. The probability scores provided by the database were retained as an indication of prediction confidence but were not used to exclude predicted targets. The resulting target list was subsequently used for downstream network and functional analyses.

2.5.1 Identification of Common Genes

We utilized the Venny2.1 (Oliveros, 2007–2015) database (https://bioinfogp.cnb.csic.es/tools/venny/) to identify common targets between the identified genes of the DHF from GEO datasets and the genes related to *A. annua* identified from Swiss target prediction.

2.5.2 Protein-Protein Interaction Network

Within cells, proteins operate by interacting with other proteins, and examining those interactions offers a deep understanding of the role of proteins (Jones & Thornton, 1996; Ben-Hur & Noble, 2005). We employed STRING v11, an online database (https://string-db.org/), to construct a network of protein-protein interactions (Szklarczyk et al., 2023). This database integrated experimental data with predicted

protein interactions to provide structural details and confidence scores. We used Cytoscape 3.10.3 software (Otasek et al., 2019) to analyze and visualize these interactions.

2.5.3 Enrichment Analysis of Key Genes

Metascape, a web-based tool (Trott & Olson, 2009) (https://metascape.org/gp/index.html#/main/step1), was used to perform enrichment analysis of common genes using the Gene Ontology (GO), KEGG, and Reactome databases, employing default statistical settings such as the Benjamini-Hochberg correction. The enriched terms were grouped into non-redundant functional clusters based on kappa-test similarity. In this study, we followed a three-step process to conduct enrichment analysis: Yap et al. (2017) performed enrichment analysis of DEGs in two different comparison groups. Sinha et al. (2024) Carried out enrichment analysis for the common genes between the two groups. Villordo et al. (2015) Executed meta-enrichment analysis for the two DEG lists.

2.5.4 Molecular Docking

Molecular docking explores various orientations and conformations of a ligand or inhibitor inside the protein binding site at the atomic level, evaluates each pose with a scoring function, and ranks them to identify the most likely binding mode (Agu et al., 2023). Molecular docking was performed to predict the binding affinity of identified bioactive compounds to receptor proteins by using AutoDock Vina software (Trott & Olson, 2009) a plugin in UCSF-Chimera (Pettersen et al., 2004). The 3 Dimensional crystal structures of identified proteins AKT1, HSP90AA1, and ESR1 were downloaded from the RCSB Protein Data Bank (Burley et al., 2023) (https://www.rcsb.org/) with PDB IDs 3O96 (Wu et al., 2010), 5CF0 (Li et al., 2015) and 1A52 (Tanenbaum et al., 1998) with resolutions of 2.70 Å, 1.80 Å, and 2.80 Å, respectively.

Before docking, the protein structures were prepared by removing water and other nonessential molecules, while retaining structurally relevant cofactors, metal ions, and other components required for protein stability or ligand binding. Missing hydrogen atoms were added, appropriate protonation states were assigned, and partial charges were calculated using the respective protein-preparation protocol. The prepared receptor structures were subsequently used for molecular docking.

The docking protocol was validated by redocking the co-crystallized ligand into its corresponding binding site. The experimentally determined binding pose of the co-crystallized ligand was compared with the predicted docking pose by calculating the root-mean-square deviation (RMSD).

For molecular docking, the binding sites were defined based on the known ligand-active-site regions of their experimentally resolved PDB structures. The docking grid was centered on the corresponding ligand-binding pocket and encompassed the residues surrounding the characterized binding site. Pymol software (Schrödinger & DeLano, 2020) (version 1.3) was used to visualize the docking results.

2.5.5 Molecular Dynamics (MD) Simulations

MD simulation is a highly reliable computational tool for investigating the dynamical interactions and motions of biomolecules (Bowers et al., 2006). In this work, docked complexes were simulated using GROMACS 2023 with the OPLS-AA force field (Abraham et al., 2015). Simulations started from the docked complexes with the highest binding affinities. Parameterization of the ligands was performed using the online Swiss-Param server, and the resulting parameters were incorporated into the GROMACS simulation protocol. Docked complexes were placed inside the appropriate solvent box and neutralized with counterions. Before the production simulation, energy minimization was performed to avoid steric clashes and obtain good initial conformations. Minimized structures were then subjected to equilibration simulations under NVT (volume and temperature constant) and NPT (pressure and temperature constant) conditions prior to starting the production run. After equilibration, the protein-ligand complexes were simulated for 100 ns of production MD under periodic boundary conditions, with temperature and pressure held constant according to the simulation parameters and coupled via the respective algorithms. The long-range electrostatics and hydrogen-bond interactions were computed using the classical GROMACS algorithms.

The trajectory analysis was used to determine stability and dynamical properties of the complexes. Conformational stability was assessed using the root-mean-square deviation (RMSD) value, whereas the flexibility of individual residues was calculated as the root-mean-square fluctuation (RMSF). The change in the compactness of the protein structure was assessed using the radius of gyration (Rg), and the number of hydrogen bonds formed between the protein and the ligand during the simulation was used as a measure of complex stability.

3 Results

3.1 Characteristics of the Selected Microarrays

Two microarray datasets, GSE18090 and GSE51808, from the NCBI-GEO database have been used to investigate differences in gene expression levels between DHF patients and normal febrile dengue-free controls (ND). GSE18090 consists of the gene expression data for blood samples of 10 DHF patients and 8 controls, whereas GSE51808 represents gene expression data for samples of circulating endothelial cells of 10 DHF patients and 9 controls. Since these datasets were generated on two different Affymetrix platforms (GPL570 for GSE18090 and GPL13158 for GSE51808), a detailed analysis of transcriptional profile alterations could be performed across different cell types associated with DHF. Differential gene expression was identified using the GEO2R tool with stringent thresholds ($|\log2 \text{ fold change}| > 1.0$ and p-value <0.05). GSE18090 resulted in 382 DEGs (289 downregulated and 93 upregulated genes). GSE51808 produced an extremely large number of DEGs, i.e., 8,777 (4,133 upregulated and 4,644 downregulated genes) (Figure 1). The findings indicate differences in the gene expression profiles of the blood and

https://doi.org/10.25135/rnp.2607.3985
Rec. Nat. Prod. 2027, 21(2):e26073985

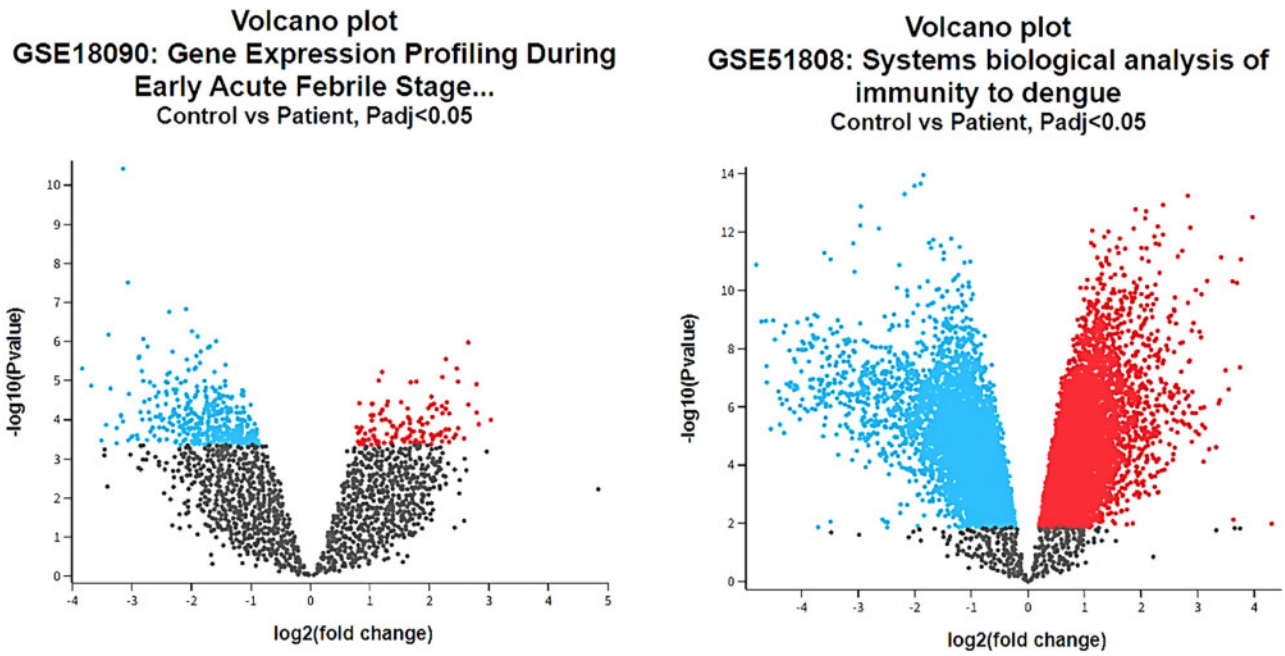


Figure 1. Volcano maps of the two datasets (GSE18090 and GSE51808). The up-regulated and down-regulated genes are indicated in red and blue dots, respectively. Black dots indicate genes with no significant difference

circulating endothelial cells of DHF patients, which can serve as molecular mechanisms underlying DHF and potential drug targets (Figure 1).

3.2 Meta-Analysis of Significant Genes

By integrating individual DEG analyses from both datasets, we identified 5, 5936, and 3837 intersecting genes within the GSE18090, GSE51808, and MetaAnalysis groups, respectively (Table 2). Our goal was to consolidate the same experimental conditions from various studies to enhance sample size and statistical power. However, because intersecting DEGs across separate studies may not always yield consistent or reproducible results, we conducted a meta-analysis to synthesize these findings. The meta-analysis identified the most reliable and stable set of genes associated with the studied pathology, thereby minimizing study-specific biases and generalizing the results. A heatmap was designed to visualize the gene expression pattern. Up-regulated and down-regulated genes separated the control group from DHF (Figure 2). Purple-colored genes in heatmaps indicate the most up- or down-regulated ones. These genes are associated with DHF and illustrate what gene alteration looks like. Visualization is important for further analysis and understanding of gene expression patterns.

3.3 Common Targets of *A. annua* and Hub Genes

Selection of drug-like compounds from the TCMSP database for *A. annua* was performed using the following criteria: OB > 30%, DL > 0.18, and molecular weight between 250 and 500 Da. Twenty compounds satisfying all these criteria were found, which have been presented in Table 3. Eight active compounds out of these were selected for prediction of molecular targets by the SwissTargetPrediction database.

Table 2. Number of genes with adjusted P-Value < threshold for each dataset and for the meta-analysis

Dataset	Significant genes
GSE18090	5
GSE51808	5936
MetaAnalysis	3837

Four hundred eighty-five targets were found for these eight compounds after eliminating the duplicate targets and non-coding proteins. As shown in Figure 3A, 93 targets were shared between *A. annua* and the 3,837 DHF genes identified in this study.

3.4 Functional Enrichment Analysis

The biological relevance of the 93 shared genes was assessed using Metascape enrichment analysis. The biological processes found to be enriched have been illustrated as bar plots (Figure 3B), where the most enriched pathways included protein phosphorylation (20 genes), positive regulation of response to external stimulus (19 genes), interleukin signaling (19 genes), inflammatory response (19 genes), and TNF-alpha signaling (19 genes). To visualize the relationships among the aforementioned enriched terms, a network was created (Figure 3C). In this network, nodes represent enriched biological processes, while edges represent functional similarities based on shared genes. Although both visualizations highlight similar enrichment terms, the bar plot focuses on statistical significance, whereas the network highlights the functional relationships among pathways. These findings suggest that compounds derived from

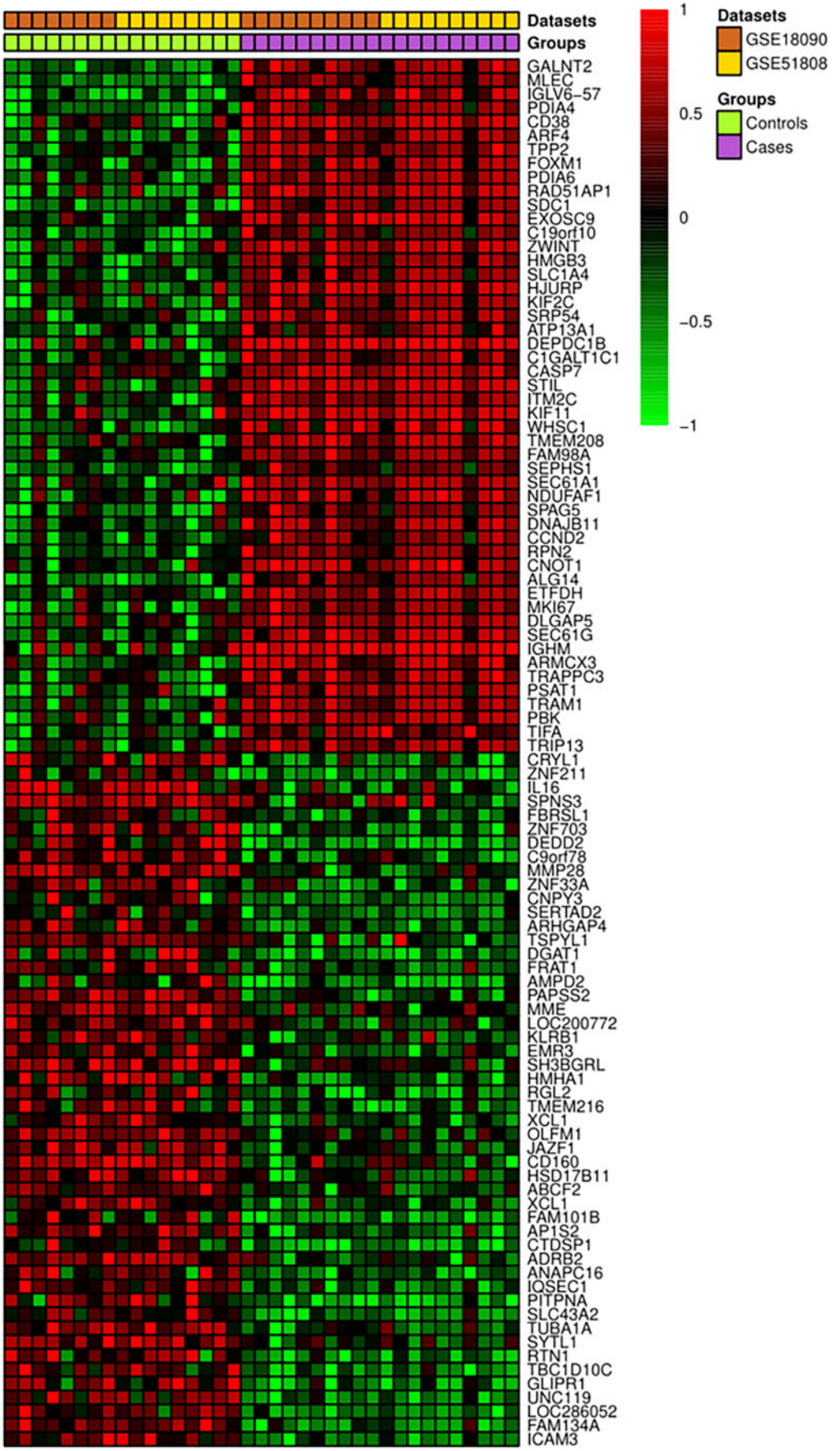


Figure 2. The heatmap diagram. DEGs clustering between the control/normal (Green color) and cases/DHF groups (Purple color)

https://doi.org/10.25135/rnp.2607.3985
Rec. Nat. Prod. 2027, 21(2):e26073985

Table 3. Summary of *A. annua*-derived compounds selected from TCMSP

MOL ID	Molecule name	Oral Bioavailability (OB)	Drug-Likeness (DL)	Molecular Weight (MW) g/mol
MOL002235	Eupatin	50.80%	0.41	360.34
MOL000354	Isorhamnetin	49.60%	0.31	316.28
MOL000359	Sitosterol	36.91%	0.75	414.79
MOL000422	Kaempferol	41.88%	0.24	286.25
MOL000449	Stigmasterol	43.83%	0.76	412.70
MOL004083	Tamarixetin	32.86%	0.31	316.28
MOL004112	Patuletin	53.11%	0.34	332.28
MOL004609	Areapillin	48.96%	0.41	360.31
MOL005229	Artemetin	49.55%	0.48	388.37
MOL000006	Luteolin	36.16%	0.25	286.25
MOL007274	Skrofulein	30.35%	0.30	314.29
MOL007389	Artemisitene	54.36%	0.31	280.32
MOL007401	Cirsiliol	43.46%	0.34	330.29
MOL007412	3,6-Dimethoxyquercetagetin (Axillarin)	42.60%	0.37	346.30
MOL007415	[(2S)-2-[[(2S)-2-(benzoylamino)-3-phenylpropanoyl]amino]-3-phenylpropyl] (Aurantiamide)	58.02%	0.52	444.45
MOL007423	6,8-di-C-glucosylapigenin	59.85%	0.21	594.50
MOL007424	Artemisinin	49.88%	0.31	282.33
MOL007425	Dihydroartemisinin	50.75%	0.30	284.35
MOL007426	Deoxyartemisinin	54.47%	0.26	266.33
MOL000098	Quercetin	46.43%	0.28	302.23

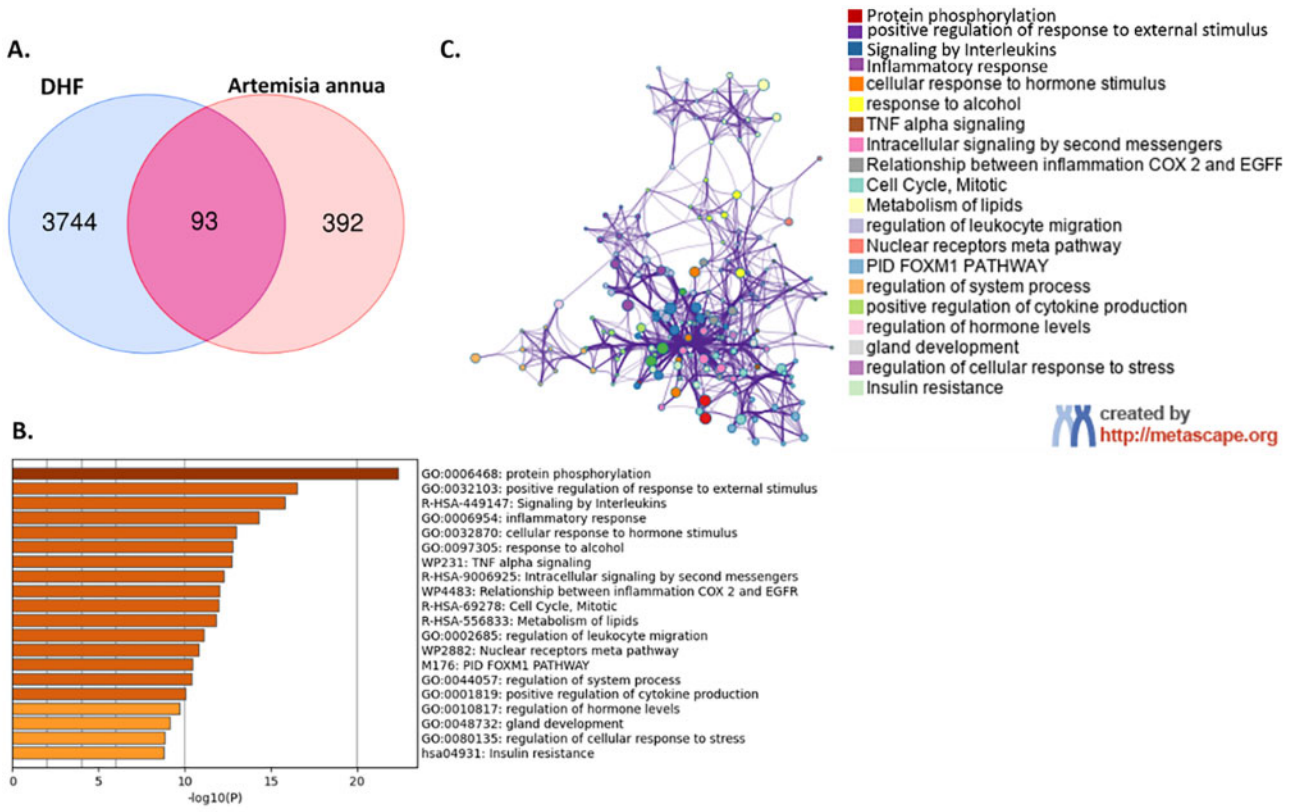


Figure 3. (A) Venn diagram showing the overlapping genes between the *A. annua* target genes and dengue hemorrhagic fever-related target genes; (B) the GO and KEGG analysis obtained by Metascape analysis; (C) Network visualization among all enriched terms

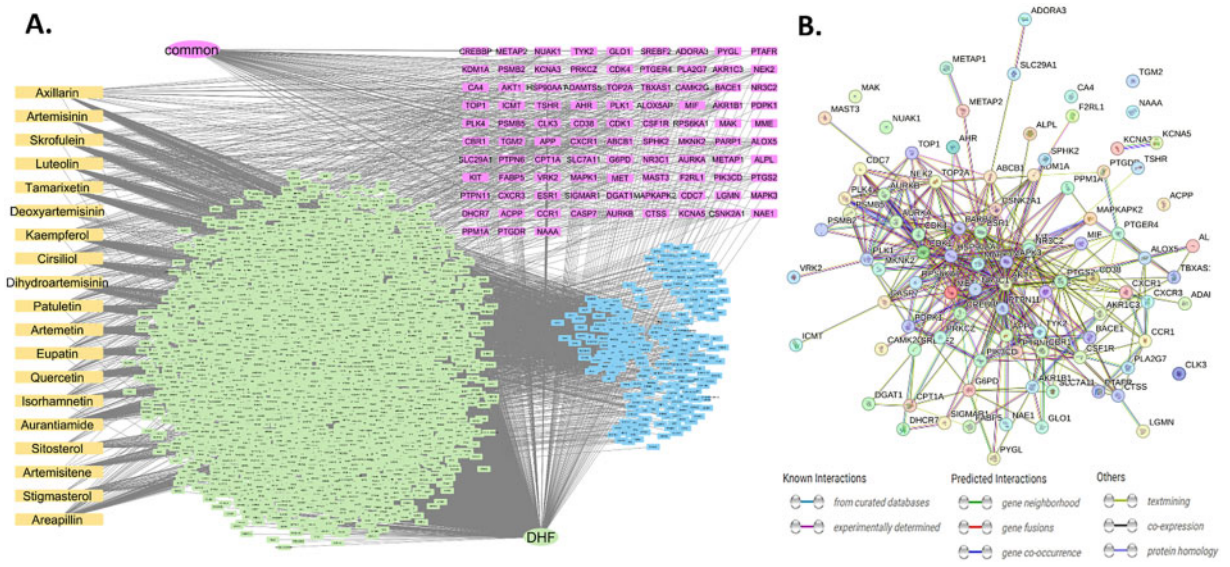


Figure 4. (A) Protein-protein interaction network comprising 93 common key molecular targets. Compounds derived from *A. annua are* shown in yellow, Genes related to DHF are shown in green, and the 93 common genes are shown in pink. (B) STRING network interaction analysis of common targets

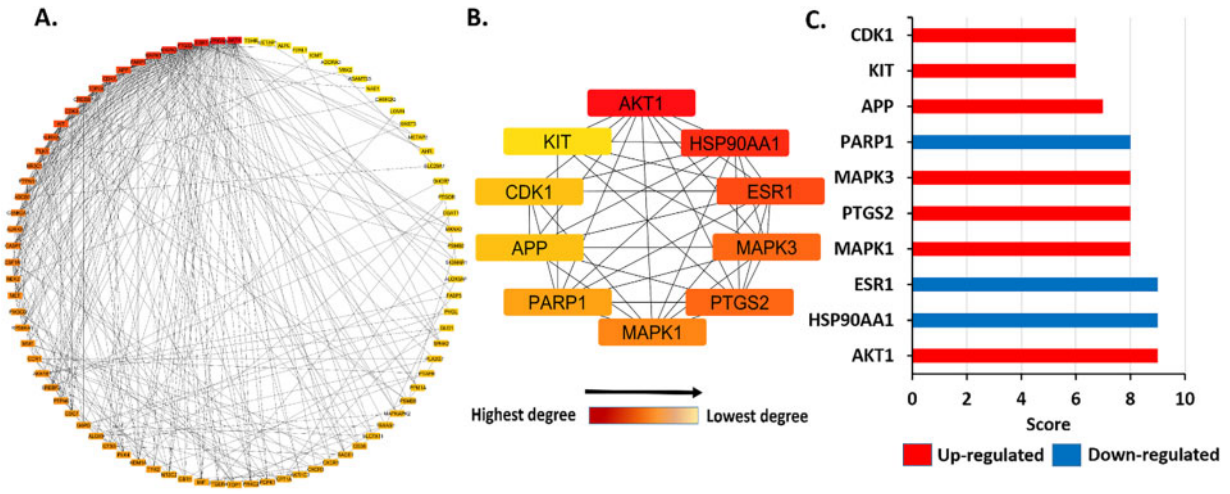


Figure 5. Network analysis of DHF genes. (A) Network analysis of anti-DHF core targets based on degree centrality. Node colors range from red (highest) to yellow (lowest) as degree decreases. (B) Top ten anti-DHF core targets. (C) The bar graph shows the top ten anti-DHF core targets

A. annua may exert anti-DHF effects by modulating inflammatory mechanisms.

3.5 Network Construction of Disease Target Proteins and Compounds

Protein interaction data for 93 core targets of *A. annua* that are effective against DHF were uploaded to Cytoscape 3.10.3 to perform a network analysis of phytochemicals, targets, and diseases. Each connection represents the relationship between bioactive compounds and target genes (Figure 4A). Additionally, we developed a PPI network for the 93 core targets shared in the fight against DHF, derived from *A. annua*. This network included 93 nodes and 366 connections (Figure 4B). Upon assessing the PPI enrichment score, we observed a clustering coefficient of 0.556, an average node degree of 7.87, and a p-value of 1.0 e−16.

Additionally, we transferred data from the STRING database into Cytoscape 3.10.3 to identify core genes by calculating their degree centrality. The analysis revealed that the primary therapeutic targets for addressing DENVI are AKT1, HSP90AA1, ESR1, MAPK1, PTGS2, MAPK3, PARP1, APP, KIT, and CDK1 (Figure 5A). Figure 5B illustrates the top ten targets, including AKT1 (RAC (Rho family)-alpha serine/threonine-protein kinase), HSP90AA1 (Heat Shock Protein 90 Alpha Family Class A Member 1), and ESR1 (Estrogen Receptor 1). Moreover, the top 10 genes were generally upregulated in DHF patients, except for HSP90AA1, ESR1, and PARP1, which were downregulated (Figure 5C).

https://doi.org/10.25135/rnp.2607.3985
Rec. Nat. Prod. 2027, 21(2):e26073985

Table 4. Docking scores in kcal/mol of *A. annua*-derived compounds against AKT1, HSP90AA1, and ESR1

Compound	PubChem ID	AKT1	HSP90AA1	ESR1
Artemisinin	68827	−10	−8.3	−8.3
Luteolin	5280445	−9.8	−9.3	−9.3
Aurantiamide	10026486	−9.8	−10.3	−10.3
Artemisitene	11000442	−9.7	−8.4	−8.4

These results suggest that these targets are closely interconnected within the network and may play important roles in the progression of DHF.

The PPI network analysis approach was used to select candidate key targets for further structural analysis. Key targets were defined as those with a high degree of connectivity in the network and a tight relationship with the specified biological processes. Candidate targets were selected for docking against selected compounds due to their biological importance and network centrality.

3.6 Molecular Docking

To investigate the binding affinity and structural stability towards AKT, HSP90AA1, and ESR1, molecular docking of the selected phytocompounds was performed. In the initial stage of the screening for binding with AKT, the docked complexes with the co-crystallized ligands were used as references, and four compounds with high binding scores were chosen: artemisinin, luteolin, aurantiamide, and artemisitene. Further analysis revealed the potential of these compounds to bind to HSP90AA1 and ESR1, thereby indicating multi-target interactions (Table 4). It was found that aurantiamide is the most effective binder (the binding scores being equal to −9.8, −10.3, and −10.3 kcal/mol for AKT, HSP90AA1, and ESR1, correspondingly), while luteolin demonstrates relatively high binding scores for all considered targets: −9.8, −9.3, and −9.3 kcal/mol for AKT, HSP90AA1, and ESR1, respectively. The investigation of the binding mode in the AKT kinase domain (Figure 6A) showed the presence of key residues stabilizing the complex at the active site of the enzyme: Val270, Leu264, Lys284/286 (Lys286 is mentioned in the text), and Leu210 (Figure 6B, 6C). Of importance is the finding that aurantiamide and artemisitene form important contacts with Asp292, the key residue of the DFG motif, which plays a role in the process of phosphorylation (Figure 6D, 6E). Moreover, the orientation of selected compounds with the N-terminal ATP-binding site of HSP90AA1 looks promising (Figure 7A), and the key residues contributing to the formation of the contact are located in a conserved cluster: Ser52, Met98, Phe138, Gly139, and Trp162 (Figures 7B–7E). Finally, the docking into the ESR1 ligand-binding site (Figures 8A–8E) showed good

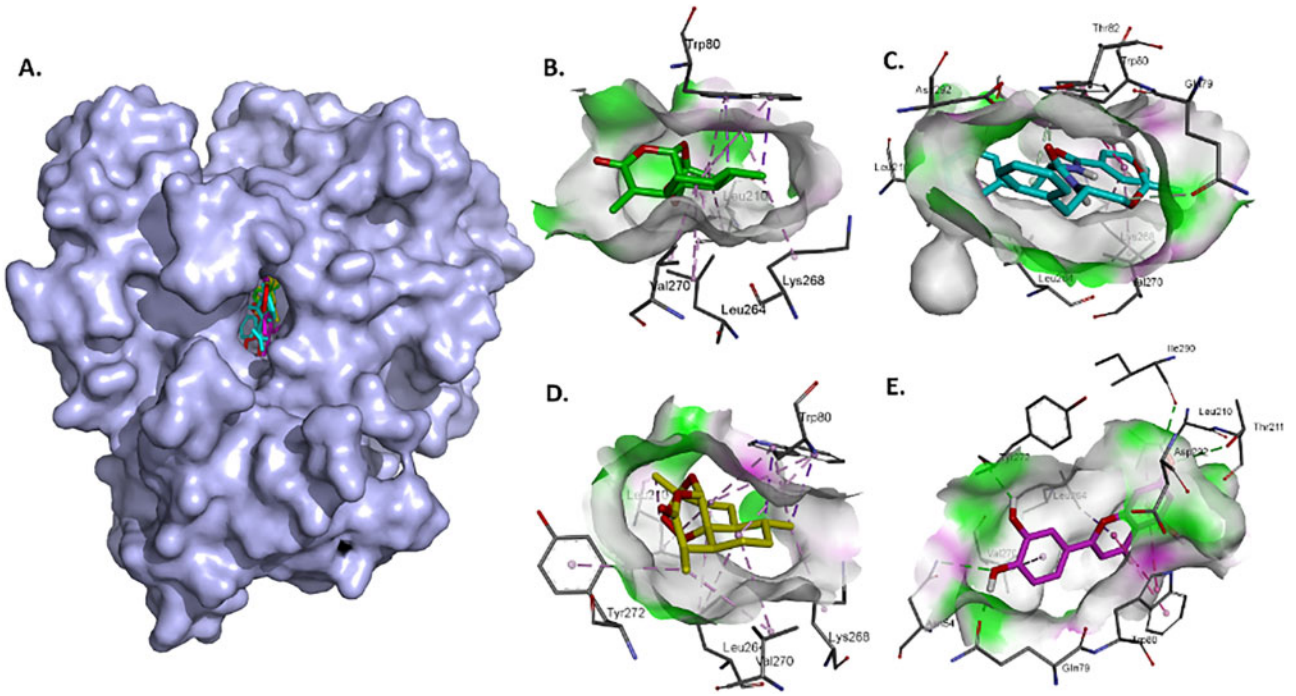


Figure 6. Docked complexes of bioactive compounds with protein AKT1 (PDB ID: 3O96). (A) Surface representation of the binding mode of compounds within the active site of AKT1. 3D binding representation of (B) Artemisinin, (C) Aurantiamide, (D) Artemisinin, (E) Luteolin

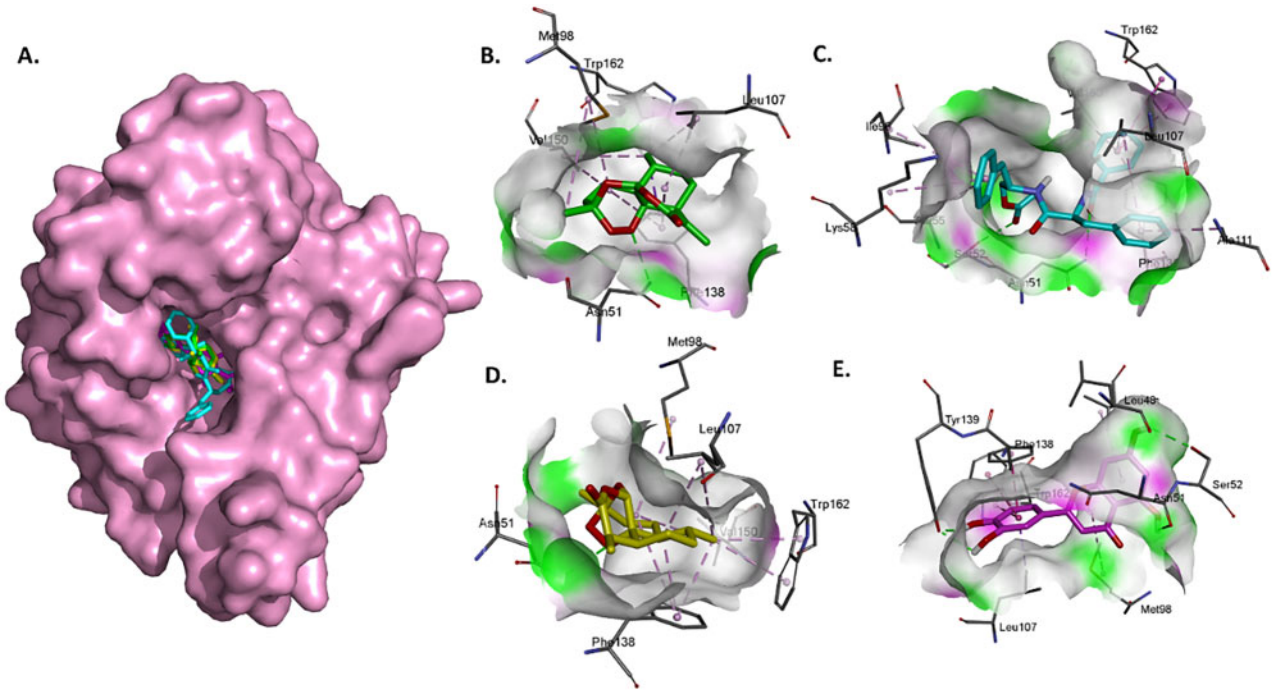


Figure 7. Docked complexes of compounds with protein HSP90AA1 (PDB ID: 5CF0). (A) Surface representation of the binding mode of compounds within the active site of HSP90AA1. 3D binding representation of (B) Artemisinin, (C) Aurantiamide, (D) Artemisinin, (E) Luteolin

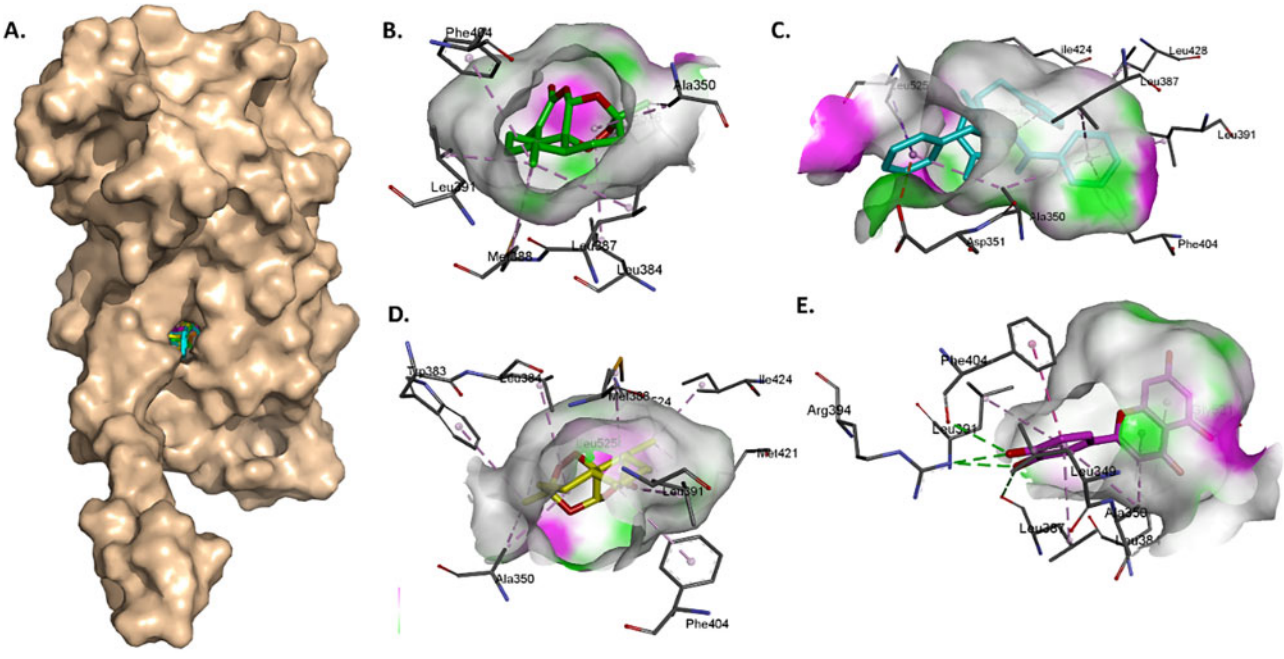


Figure 8. The docked complexes of compounds with the ESR1 protein (PDB ID: 1A52). (A) Surface representation of the binding mode of compounds within the active site of ESR1. 3D binding representation of (B) Artemisinin, (C) Aurantiamide, (D) Artemisinin, (E) Luteolin

structural compatibility, provided by the formation of contacts with Ala350, Phe404, and Ile424 in the active-site cavity. Therefore, the selected compounds demonstrate good binding properties and can modulate the biological activity of these key proteins by interacting with their catalytic and regulatory domains.

The reliability of the molecular docking protocol was evaluated by redocking the co-crystallized ligands into their respective binding sites. The RMSD values obtained for 3O96, 5CF0, and 1A52 were 1.80 Å, 1.27 Å, and 0.28 Å, respectively. The obtained RMSD values indicated satisfactory reproduction of the experimentally determined

https://doi.org/10.25135/rnp.2607.3985
Rec. Nat. Prod. 2027, 21(2):e26073985

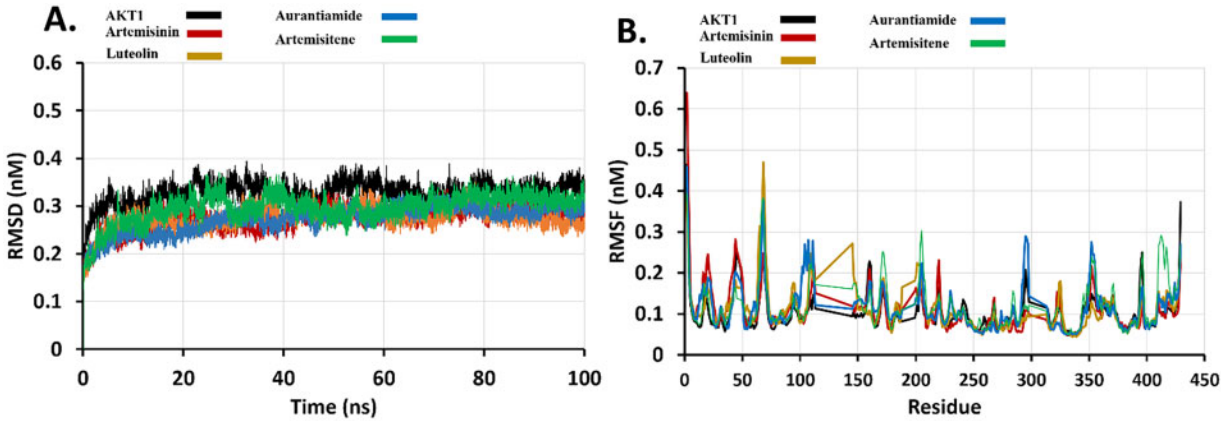


Figure 9. MDS analysis of binding behavior of compounds in complex with AKT1 for a total of 100 ns. (A) Root mean square deviations (RMSD). (B) Root mean square fluctuation (RMSF)

ligand-binding conformations, supporting the reliability of the docking protocol for subsequent analysis.

3.7 Molecular Dynamics Simulations

Simulations were performed over 100 ns to assess compound stability against three primary core targets: AKT1, ESR1, and HSP90AA1. For AKT1, the compound complexes exhibited a lower Root Mean Square Deviation (RMSD) compared to the apo protein, indicating that ligand binding results in a structural tightening, thereby stabilizing the protein's overall conformation (Figure 9A). The peaks in the RMSF for residues 110 to 150, especially when Luteolin is present, are considered to be either flexible loops or induced fit in distal regions (Figure 9B). The affinity of the ligand Aurantiamide is supported by hydrogen bonds (with up to eight possible hydrogen bonds) and the stability of active site residues (Figure 10A, B).

The RMSD fluctuations in the case of the Aurantiamide-ESR1 complex were significant but transient, occurring between 35 and 58 ns, with RMSD values ranging from 2.7 to 2.8 nM (Figure 11A). Such a deviation indicates a significant conformational change in the complex due to changes in ESR1 ligand orientation. Later on, the RMSD value dropped to a significantly more stable level, suggesting that such deviation is temporary and there is no sign of progressive instability of the complex or ligand dissociation. Nevertheless, this fluctuation indicates a period of reduced conformational stability and should be considered when interpreting the overall binding behavior of Aurantiamide with ESR1 and Artemisitene (90–97 ns) (Figure 11A), along with increasing RMSF values (Figure 11B), suggest a "conformational breathing" mechanism or a temporary shift in the binding pose where the ligand explores a local energetic minimum before returning to a stable equilibrium. These fluctuations in ESR1 may also result from the ligands' interaction with highly mobile helices (such as Helix 12), where the high number of hydrogen bonds for Luteolin (up to 14) implies a very rigid anchoring compared to the more dynamic behavior of Aurantiamide and Artemisitene (Figure 12A, B). Finally, simulations of HSP90AA1 showed largely conserved structural integrity across all complexes (Figure 13A, B). However, significant Ligand-RMSD fluctuations for Luteolin between 30–50 ns indicate a period of rotational or translational adjustment within the hydrophobic pocket, eventually reaching a stable state supported by an extensive hydrogen-bonding network (up to 12 bonds) (Figure 14A, B). Overall, the simulations demonstrate that while specific compounds exhibit localized transient instability, the high hydrogen-bond occupancy and comparable RMSD profiles relative to the apo proteins support the potential of these compounds as stable inhibitors of the target genes.

Thus, the molecular dynamics results support high-affinity binding, as predicted by molecular docking, and these compounds exhibit high docking scores and good structural complementarity within the catalytic and regulatory domains of AKT1, ESR1, and HSP90AA1. It seems that the "tightening" of the structure of AKT1, due to residues like Asp292, along with the RMSD/RMSF changes observed for ESR1 and HSP90AA1, may represent an optimization of the orientation of these ligands in the Ala350- and Phe404-rich pockets, which is the transition from a static docking pose to a 100 ns dynamic equilibrium. The fluctuations, including the conformational "breathing" of ESR1 and rearrangement of the luteolin position in HSP90AA1, resulted in the formation of a stable hydrogen-bond network (up to 14 bonds), demonstrating that phytocompounds extracted from *A. annua* can have a stable inhibitory effect on multiple targets over time.

The docking and molecular dynamics simulations showed that the selected compounds interacted with key residues in the binding pockets of the targeted proteins. The interactions involved hydrogen bonding, hydrophobic interactions, and π-π interactions, some of which were stable during the MD simulation. Further analysis of RMSD, RMSF, radius of gyration, and hydrogen bonding confirmed the stability of the protein-ligand complex structures. However, these computational results show only binding affinity, not inhibition. They should be experimentally validated.

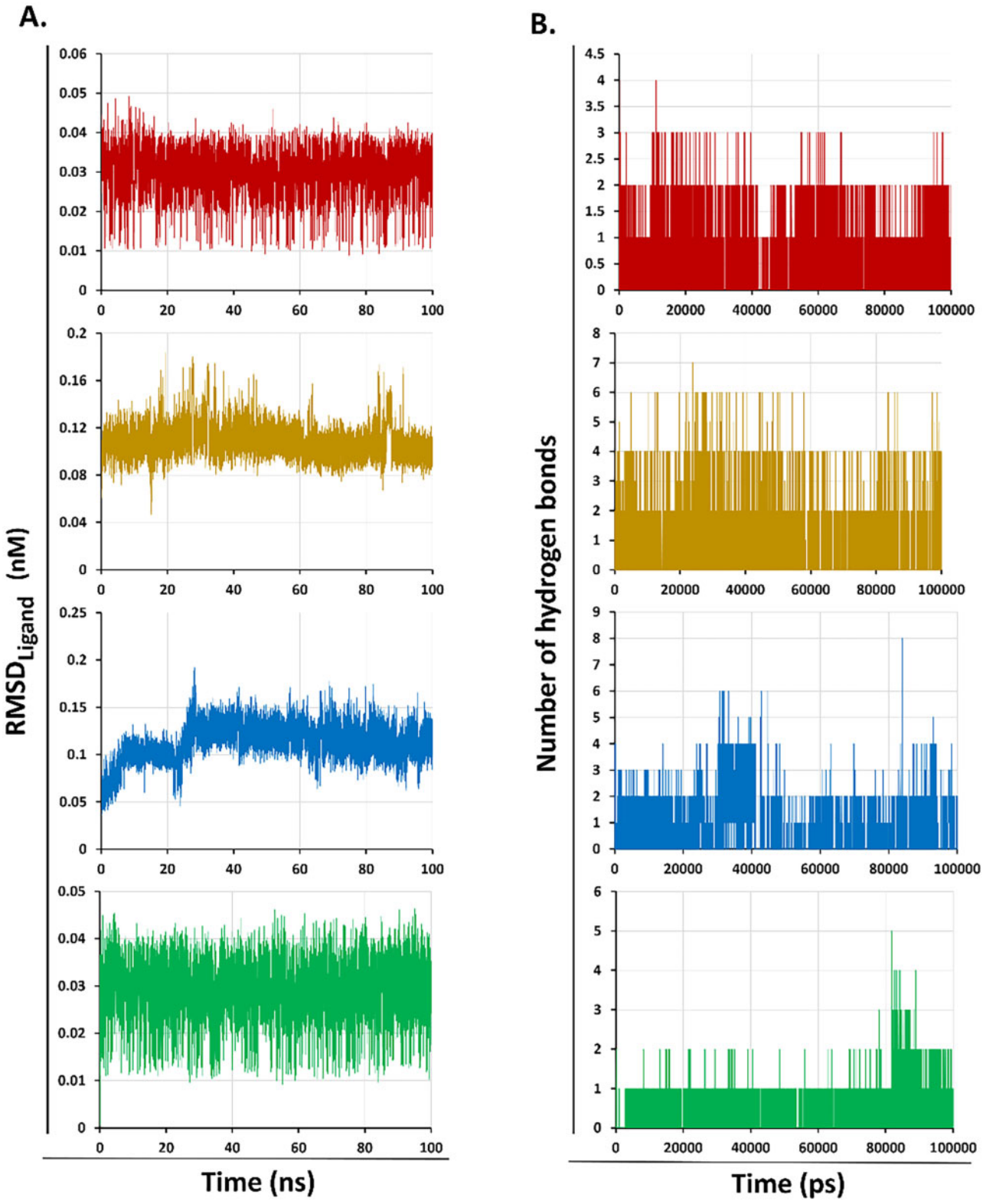


Figure 10. Analysis of (A) RMSD of ligands and (B) number of hydrogen bonds formation for compounds-AKT1 complexes for a total of 100 ns. Artemisinin (red), Luteolin (yellow), Aurantiamide (blue), Artemisitene (green)

https://doi.org/10.25135/rnp.2607.3985
Rec. Nat. Prod. 2027, 21(2):e26073985

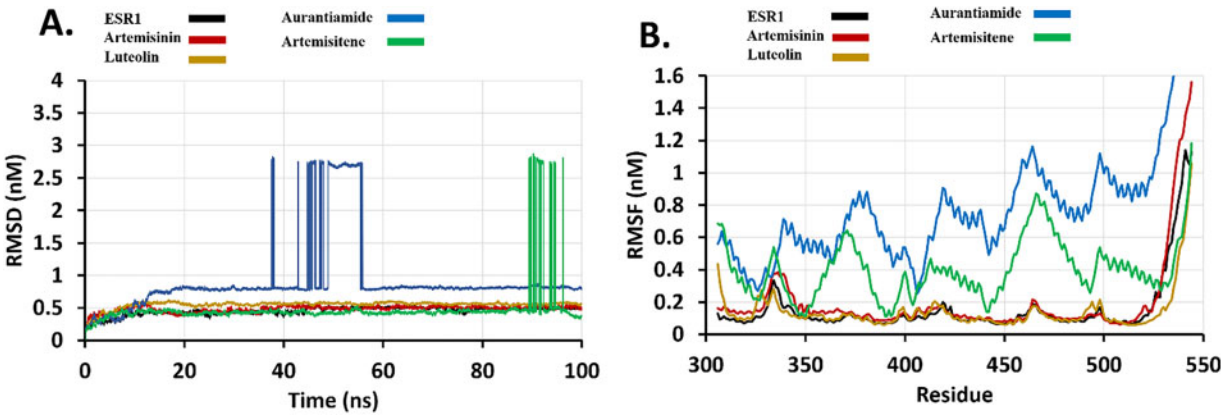


Figure 11. MDS analysis of the binding behavior of compounds in complex with ESR1 for a total of 100 ns. (A) Root mean square deviations (RMSD). (B) Root mean square fluctuation (RMSF)

4 Discussion

Dengue fever is a significant global health challenge due to its widespread prevalence and potential to cause severe illness, including complications such as dengue hemorrhagic fever and dengue shock syndrome (Gubler, 2006; Kalayanarooj, 2011). Despite the high burden of dengue, current research efforts have yet to fully elucidate the complex interactions between the dengue virus and host cellular mechanisms, particularly the identification of key host genes that drive dengue virus infection (Khan et al., 2025). Researchers have increasingly employed bioinformatics approaches to identify novel and potential biosignatures and understand the mechanisms causing dengue (Latif et al., 2025; Al Noman et al., 2025). These computational methods enable the analysis of large-scale genomic and transcriptomic datasets, facilitating the detection of differentially expressed genes and key regulatory networks involved in the host response to dengue virus infection. By incorporating multiple forms of data, which include gene expression, protein interactions, pathway associations, network pharmacology, and bioactive compounds, it is possible to create an approach to identifying critical host factors affecting disease severity and progression (Khan et al., 2025; Khetarpal & Khanna, 2016; Screaton et al., 2015). Overall, the integration of bioinformatics tools accelerates the translation of molecular discoveries into clinical practice and improves patient treatment and management. In the current study, two datasets from NCBI-GEO (GSE18090 and GSE51808) were analyzed to identify the most important molecular biomarkers in DENVI. Using the TCMSP database, bioactive compounds from *A. annua* were analyzed, and, according to preset criteria, compounds suitable for drug development were selected. For each bioactive compound, target genes were specified, and based on these, 93 common targets in *A. annua* and genes from the GEO datasets were identified.

Using functional enrichment analysis, the following pathways were highlighted among the 93 overlapping genes between DENVI and bioactive compounds of *A. annua*: protein phosphorylation, interleukin signaling pathway, inflammatory response, and TNF-α signaling pathway. These results coincide with the hyperinflammation described in DENVI and can provide insight into genes that could serve as targets to reduce disease severity. Using network pharmacology and protein-protein interaction analysis, AKT1, HSP90AA1, and ESR1 were determined as core genes potentially involved in the disease progression. AKT1 is a serine/threonine kinase that plays a significant role in cell survival and immune regulation (Rogers, 2026; Ho et al., 2014). The AKT1 gene is situated on chromosome 14q32.33 and encodes a protein with a kinase domain, an N-terminal pleckstrin homology domain, and a C-terminal regulatory domain. Activation occurs through phosphorylation at Thr308 and Ser473 after PI3K generates PIP3, thereby recruiting the protein to the cell membrane. This gene has several splice variants and is highly conserved across species (NIH, 2026). HSP90AA1 encodes the stress-inducible isoform of heat shock protein 90 alpha (Hsp90α), a key molecular chaperone that assists in the folding, stabilization, and activation of client proteins under cellular stress. Located on chromosome 11q21, HSP90AA1 encodes a 90-kDa protein that functions as a homodimer and relies on ATP hydrolysis for its chaperone cycle, which involves conformational changes. Unlike its constitutive paralog HSP90AB1 (Hsp90β), HSP90AA1 expression surges under proteotoxic stress such as heat shock, increasing up to 7-fold (Lv et al., 2025; Wan et al., 2025), and is involved in protein folding and stress responses. ESR1 modulates inflammatory and immune signaling. ESR1 encodes estrogen receptor alpha (ERα), a nuclear receptor that binds estrogen to regulate gene transcription in reproductive, metabolic, and developmental processes. ESR1 is located on chromosome 6q25.1 and produces a protein with an N-terminal AF-1 transactivation domain, a DNA-binding domain, a hinge region, and a C-terminal ligand-binding domain with AF-2 (ScienceDirect, 2015). The differential expression patterns observed—upregulation of AKT1 and downregulation of HSP90AA1 and ESR1—may reflect complex regulatory dynamics during DHF.

Molecular docking and 100 ns molecular dynamics simulations demonstrated that *A. annua* compounds—

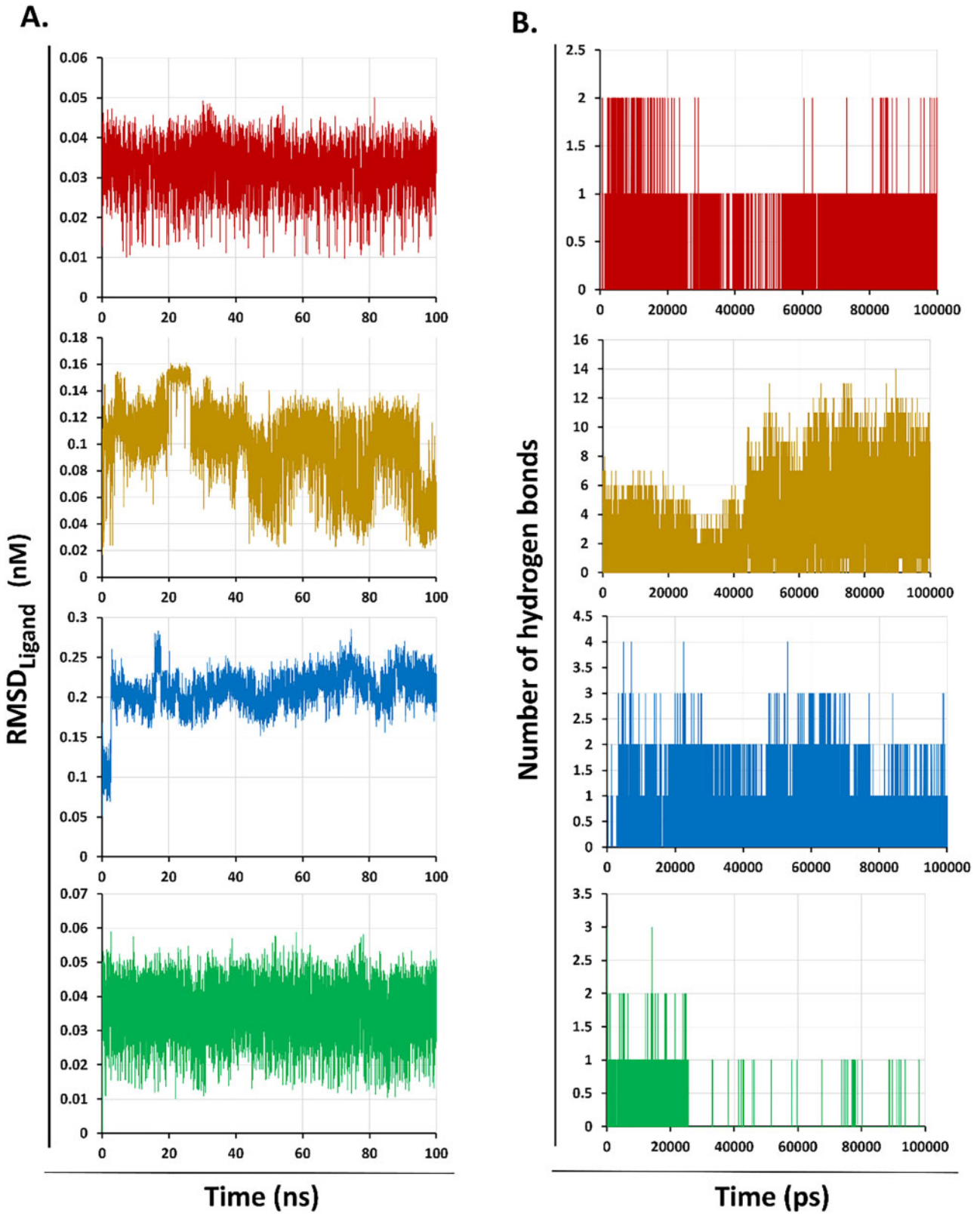


Figure 12. Analysis of (A) RMSD of ligands and (B) number of hydrogen bond formations for compounds-ESR1 complexes for a total of 100 ns. Artemisinin (red), Luteolin (yellow), Aurantiamide (blue), Artemisitene (green)

https://doi.org/10.25135/rnp.2607.3985
Rec. Nat. Prod. 2027, 21(2):e26073985

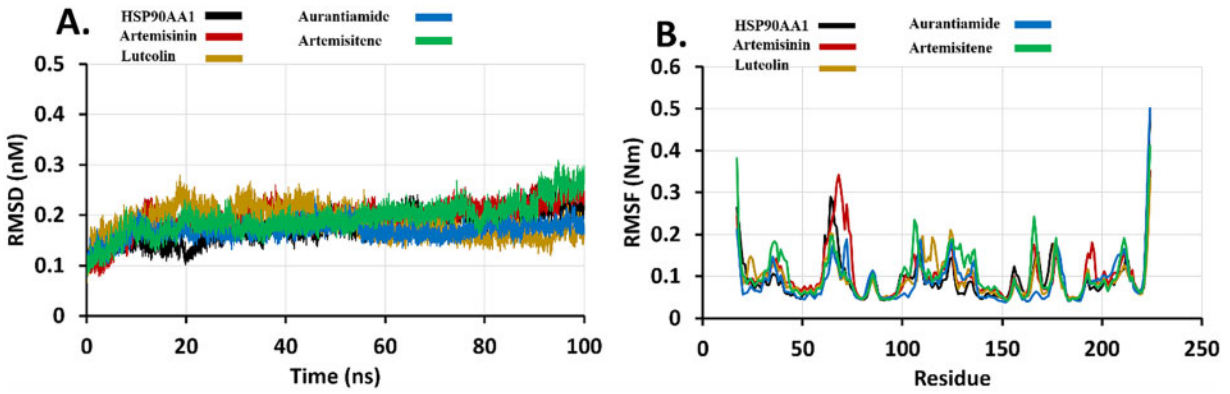


Figure 13. MDS analysis of binding behavior of compounds in complex with Hsp90-alpha for a total of 100 ns. (A) Root mean square deviations (RMSD). (B) Root mean square fluctuation (RMSF)

Artemisinin, Luteolin, Aurantiamide, and Artemisitene—exhibit strong binding affinity and stable interactions with these hub proteins. Significantly, Aurantiamide showed strong binding to all targets, interacting with crucial protein residues. MD studies revealed that the relevant proteins were stable over long timescales, and hydrogen-bond formation and conformational changes supported the probable inhibitory action. The observed "conformational breathing" and transient fluctuations in ESR1 and HSP90AA1 complexes suggest dynamic ligand accommodation, which may be advantageous for modulating protein activity.

Artemisinin is a sesquiterpene lactone primarily used to treat malaria by activating the endoperoxide bridge via heme iron, generating reactive oxygen species (ROS). Beyond parasites, it shows anticancer effects by inducing apoptosis, cell cycle arrest, and inhibiting angiogenesis in various cancers, plus activity against schistosomiasis and viruses like herpes (Rogers, 2026; Ho et al., 2014).

Luteolin, a flavonoid in vegetables and fruits, exerts anti-inflammatory, antioxidant, and antiviral effects by inhibiting PI3K/AKT/NF-κB, MAPK, and promoting Treg function (Lv et al., 2025). It alleviates pulmonary diseases and atherosclerosis via lipid reduction and inhibition of apoptosis, and RSV/SARS-CoV-2 infections by blocking ACE2 and oxidative stress (Wan et al., 2025). Aurantiamide (often as the acetate from *Portulaca oleracea*) exerts anti-inflammatory effects by suppressing NF-κB and MAPK (p38/JNK) phosphorylation and reducing pro-inflammatory cytokines (Chen et al., 2016). It exhibits anticancer, antiviral, and rapid-absorption pharmacokinetics, with tissue distribution peaking early and minimal accumulation (Chen et al., 2016). Artemisinin and its derivatives share endoperoxide mechanisms of ROS-mediated cytotoxicity against parasites and cancers, though they have been studied less independently. It contributes to the effects of the artemisinin family on autoimmune, allergic, and septic models by inhibiting TLR, Syk, and STAT (Ho et al., 2014). These findings provide a computational foundation for the multi-target inhibitory potential of *A. annua* derivatives in attenuating the hyperinflammatory response characteristic of DHF. By targeting central nodes in inflammatory signaling, these compounds may offer a novel therapeutic strategy addressing both viral replication and host immune dysregulation.

Several recent studies demonstrated that a small-molecule compound possesses antiviral effects against various types of flaviviruses, namely DENV, ZIKV, and JEV, demonstrating the potential for more generalized treatment approaches (Zhang et al., 2020; Joe et al., 2022; Zhu et al., 2023). The compound acts as an antagonist of DENV-mediated changes in endothelial cells, restoring junctional proteins, reducing mesenchymal markers, and preventing viral entry and infection. Thus, it seems like the compound is able to mitigate the mechanisms responsible for the development of severe dengue pathology (Escudero-Flórez et al., 2023; Schor & Einav, 2018). QL47 is a novel small-molecule antiviral inhibitor affecting the host cell. It blocks BTK kinase activity and translation of the virus, which hinders the molecular processes in the replication cycle of positive-sense RNA viruses (Liang et al., 2017; De Wispelaere et al., 2017; De Wispelaere et al., 2020).

Overall, the combination of bioinformatics and molecular simulation methods enabled us to identify pivotal molecular targets and potentially beneficial compounds from *A. annua* with anti-DHF activity. These results will serve as the basis for further experimental research.

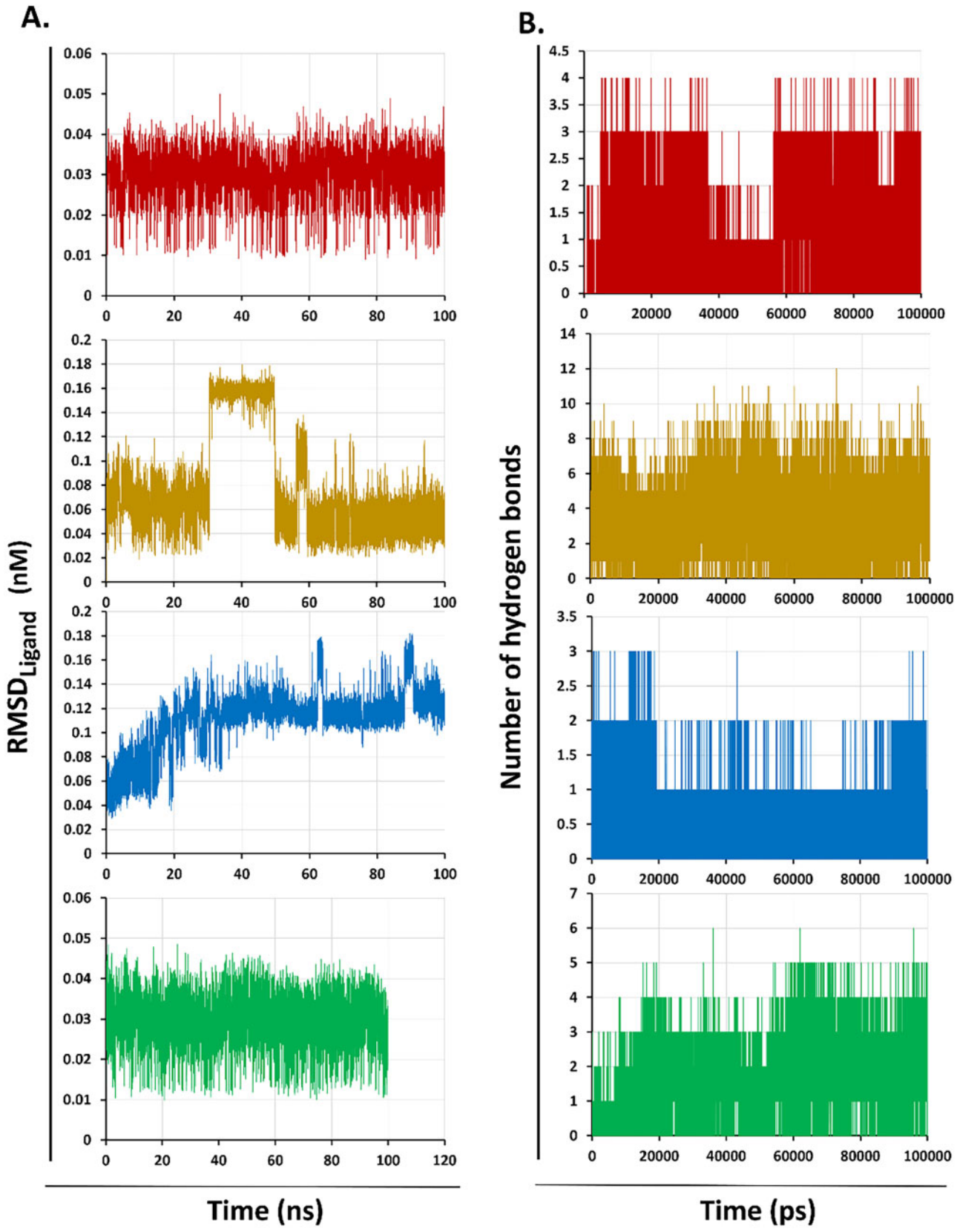


Figure 14. Analysis of (A) RMSD of ligands and (B) number of hydrogen bond formations for compounds-Hsp90-alpha complexes for a total of 100 ns. Artemisinin (red), Luteolin (yellow), Aurantiamide (blue), Artemisitene (green)

https://doi.org/10.25135/rnp.2607.3985
Rec. Nat. Prod. 2027, 21(2):e26073985

5 Conclusion

The present work employs bioinformatics and computational approaches to identify key hub genes associated with DHF and to evaluate the antiviral potential of compounds isolated from *A. annua*. Transcriptomic dataset analysis has identified 93 common targets for DHF and active ingredients of *A. annua*. These targets were found to be involved in inflammation and immune-related pathways. Network pharmacology and protein-protein interaction analyses have identified the hub genes AKT1, HSP90AA1, and ESR1.

Among the four studied compounds, Aurantiamide exhibited the highest overall performance due to strong docking with HSP90AA1 and ESR1, as well as stable molecular interactions over 100 ns of molecular dynamics simulation. Luteolin was also found to exhibit strong dynamic interactions, primarily due to hydrogen-bond networks with ESR1 and HSP90AA1. Based on the results obtained, Aurantiamide can be regarded as the best compound from *A. annua* for DHF due to its ability to modulate hyperinflammation. This study provides computational evidence of the multi-target inhibitory capacity of phytocompounds isolated from *A. annua* against DHF-associated mechanisms.

It should be noted that the current work is limited to in silico analysis. Thus, experimental evaluation of the phytocompounds is needed to confirm their antiviral capacity, pharmacodynamics, and safety profiles. In addition, it would be important to study pharmacokinetics and synergy of these phytochemicals.

Acknowledgement

The author extend their appreciation to Prince Sattam bin Abdulaziz University for funding this research work through the project number (PSAU/2026/03/45875).

Funding Statement

This work was supported by Prince Sattam bin Abdulaziz University under Grant number (PSAU/2026/03/45875).

Author Contributions

M.A. contributed to the conceptualization, methodology, data collection, analysis, and interpretation of the study and drafted the manuscript. M.K. contributed to the study design, data interpretation, manuscript review, and critical revision. Both authors approved the final version of the manuscript and agreed to be accountable for all aspects of the work.

Availability of Data and Materials

The authors declare that should any raw data files be needed about the further data of the study, they are available from the corresponding author upon reasonable request. Source data are provided with this paper.

Artificial Intelligence (AI) Statement

The authors utilized Gemini 3 for enhancing language and correcting grammatical errors. All content generated with the assistance of AI was thoroughly reviewed, verified, and sanctioned by the authors, who assume complete responsibility for the precision and integrity of the final manuscript.

Conflicts of Interest

The authors declare that they do not have any conflict of interest.

ORCID

Mubarak A. Alamri: 0000-0003-0678-593x
Mohamed Ahmed Akela: 0000-0002-5620-1907

References

Abraham, M. J., Murtola, T., Schulz, R., Páll, S., Smith, J. C., Hess, B. & Lindahl, E. (September 2015). GROMACS: High performance molecular simulations through multi-level parallelism from laptops to supercomputers. *SoftwareX*, *1–2*, 19–25. DOI: 10.1016/j.softx.2015.06.001.

Agu, P. C., Afiukwa, C. A., Orji, O. U., Ezeh, E. M., Ofoke, I. H., Ogbu, C. O., Ugwuja, E. I. & Aja, P. M. (August 17, 2023). Molecular docking as a tool for the discovery of molecular targets of nutraceuticals in diseases management. *Scientific Reports*, *13*(1), 13398. DOI: 10.1038/s41598-023-40160-2.

Al Noman, M., Latif, M. A., Ahmed, M. F., Islam, M. S., Al Amin Pappu, M., Hossain, M. S., Hossen, M. B., Noor, T., Mollah, M. M. H., Kabir, M. H. & Mollah, M. N. H. (November 11, 2025). In-silico discovery of druggable molecular signatures that drive dengue fever to severe dengue fever highlighting common pathogenesis through single-cell RNA-Seq analysis. *Scientific Reports*, *15*(1), 39449. DOI: 10.1038/s41598-025-23000-3.

Baggieri, M., Gioacchini, S., Borgonovo, G., Catinella, G., Marchi, A., Picone, P., Vasto, S., Fioravanti, R., Bucci, P., Kojouri, M., Giuseppetti, R., D'Ugo, E., Ubaldi, F., Dallavalle, S., Nuzzo, D., Pinto, A. & Magurano, F. (December 2023). Antiviral, virucidal and antioxidant properties of *A. annua* against SARS-CoV-2. *Biomedicine & Pharmacotherapy*, *168*, 115682. DOI: 10.1016/j.biopha.2023.115682.

Barrett, T. (December 17, 2004). NCBI GEO: Mining millions of expression profiles–database and tools. *Nucleic Acids Research*, *33*(Database issue), D562–D566. DOI: 10.1093/nar/gki022.

Ben-Hur, A. & Noble, W. S. (June 1, 2005). Kernel methods for predicting protein-protein interactions. *Bioinformatics*, *21*(Suppl 1), i38–i46. DOI: 10.1093/bioinformatics/bti1016.

Bowers, K. J., Sacerdoti, F. D., Salmon, J. K., Shan, Y., Shaw, D. E., Chow, E., Xu, H., Dror, R. O., Eastwood, M. P., Gregersen, B. A., Klepeis, J. L., Kolossvary, I. & Moraes, M. A. (2006). Molecular dynamics—scalable algorithms for molecular dynamics simulations on commodity clusters. Proceedings of the 2006 ACM/IEEE Conference on Supercomputing-SC '06 [Internet], Tampa, Florida: ACM Press, 84. DOI: 10.1145/1188455.1188544.

Brady, O. J., Gething, P. W., Bhatt, S., Messina, J. P., Brownstein, J. S., Hoen, A. G., Moyes, C. L., Farlow, A. W., Scott, T. W. & Hay,

S. I. (August 7, 2012). Refining the global spatial limits of dengue virus transmission by evidence-based consensus. Reithinger R, editor. *PLOS Neglected Tropical Diseases*, *6*(8), e1760. DOI: 10.1371/journal.pntd.0001760.

Burley, S. K., Bhikadiya, C., Bi, C., Bittrich, S., Chao, H., Chen, L., Craig, P. A., Crichlow, G. V., Dalenberg, K., Duarte, J. M., Dutta, S., Fayazi, M., Feng, Z., Flatt, J. W., Ganesan, S., Ghosh, S., Goodsell, D. S., Green, R. K., Guranovic, V., Henry, J. (January 6, 2023). RCSB protein data bank (RCSB.org): Delivery of experimentally-determined PDB structures alongside one million computed structure models of proteins from artificial intelligence/machine learning. *Nucleic Acids Research*, *51*(D1), D488–D508. DOI: 10.1093/nar/gkac1077.

Chauhan, N., Gaur, K. K., Asuru, T. R. & Guchhait, P. (August 28, 2024). Dengue virus: Pathogenesis and potential for small molecule inhibitors. *Bioscience Reports*, *44*(8), BSR20240134. DOI: 10.1042/BSR20240134.

Chen, L., Liu, Y., Jia, D., Yang, J., Zhao, J., Chen, C., Liu, H. & Liang, X. (May 4, 2016). Pharmacokinetics and biodistribution of aurantiamide and aurantiamide acetate in rats after oral administration of Portulaca oleracea L. extracts. *Journal of Agricultural and Food Chemistry*, *64*(17), 3445–3455. Epub 2016 Apr 21. PMID: 27075043. DOI: 10.1021/acs.jafc.6b00470.

Choudhury, K. R., Verma, P., Ray, A. G., Samanta, S., Manna, A., Bandyopadhyay, A., Dutta, S. & Sadhukhan, P. C. (September 6, 2024). Differential proteomic profiling at different phases of dengue infection: An intricate insight from proteins to pathogenesis. *Journal of Proteome Research*, *23*(9), 3731–3745. DOI: 10.1021/acs.jproteome.3c00751.

Daina, A., Michielin, O. & Zoete, V. (2019). SwissTargetPrediction: Updated data and new features for efficient prediction of protein targets of small molecules. *Nucleic Acids Research*, *47*(W1), W357–W364. DOI: 10.1093/nar/gkz382.

De Wispelaere, M., Carocci, M., Burri, D. J., Neidermyer, W. J., Olson, C. M., Roggenbach, I., Liang, Y., Wang, J., Whelan, S. P. J., Gray, N. S. & Yang, P. L. (February 2020). A broad-spectrum antiviral molecule, QL47, selectively inhibits eukaryotic translation. *Journal of Biological Chemistry*, *295*(6), 1694–1703. DOI: 10.1074/jbc.RA119.011132.

De Wispelaere, M., Carocci, M., Liang, Y., Liu, Q., Sun, E., Vetter, M. L., Wang, J., Gray, N. S. & Yang, P. L. (March 2017). Discovery of host-targeted covalent inhibitors of dengue virus. *Antiviral Research*, *139*, 171–179. DOI: 10.1016/j.antiviral.2016.12.017.

Devignot, S., Sapet, C., Duong, V., Bergon, A., Rihet, P., Ong, S., Lorn, P. T., Chroeung, N., Ngeav, S., Tolou, H. J., Buchy, P. & Couissinier-Paris, P. (July 20, 2010). Genome-wide expression profiling deciphers host responses altered during dengue shock syndrome and reveals the role of innate immunity in severe dengue. Bozza PT, editor. *PLoS One*, *5*(7), e11671. DOI: 10.1371/journal.pone.0011671.

Escudero-Flórez, M., Torres-Hoyos, D., Miranda-Brand, Y., Boudreau, R. L., Gallego-Gómez, J. C. & Vicente-manzanares, M. (2023). Dengue virus infection alters inter-endothelial junctions and promotes endothelial–mesenchymal-transition-like changes in human microvascular endothelial cells. *Viruses*, *15*(7), 1437. DOI: 10.3390/v15071437.

Gubler, D. J. (August 25, 2006). Dengue/dengue haemorrhagic fever: History and current status. New Treatment Strategies for Dengue and Other Flaviviral Diseases: Novartis Foundation Symposium 277, Chichester, UK: John Wiley & Sons, Ltd, 3–22.

Ho, W. E., Peh, H. Y., Chan, T. K. & Wong, W. S. (April 2014). Artemisinins: Pharmacological actions beyond anti-malarial. *Pharmacology & Therapeutics*, *142*(1), 126–139. Epub 2013 Dec 6. PMID: 24316259. DOI: 10.1016/j.pharmthera.2013.12.001.

Joe, S., Salam, A. A. A., Neogi, U., N, N. B. & Mudgal, P. P. (April 2022). Antiviral drug research for Japanese encephalitis: An updated review. *Pharmacological Reports*, *74*(2), 273–296. DOI: 10.1007/s43440-022-00355-2.

Jones, S. & Thornton, J. M. (January 9, 1996). Principles of protein-protein interactions. *Proceedings of the National Academy of Sciences*, *93*(1), 13–20. DOI: 10.1073/pnas.93.1.13.

Josyula, J. V. N., Talari, P., Pillai, A. K. B. & Mutheneni, S. R. (March 2023). Analysis of gene expression profile for identification of novel gene signatures during dengue infection. *Infectious Medicine*, *2*(1), 19–30. DOI: 10.1016/j.imj.2023.02.002.

Kalayanarooj, S. (2011). Clinical manifestations and management of dengue/DHF/DSS. *Tropical Medicine and Health*, *39*(Suppl 4), S83–S87. DOI: 10.2149/tmh.2011-S10.

Kalyan, G. U., Pranathi Reddy, D., Chandrakanth, G., Pooja, B., Anitha, V. & Vivek, D. (2023). Gene association disease prediction by GEO2R tool. 2023 International Conference on Evolutionary Algorithms and Soft Computing Techniques (EASCT) [Internet], Bengaluru, India: IEEE, 1–6. [cited 2025 Dec 21]. DOI: 10.1109/EASCT59475.2023.10392802.

Khan, M. A. A., Zilani, M. N. H., Hasan, M. & Hasan, N. (February 2025). Identification and evaluation of bioactive compounds from Azadirachta indica as potential inhibitors of DENV-2 capsid protein: An integrative study utilizing network pharmacology, molecular docking, molecular dynamics simulations, and machine learning techniques. *Heliyon*, *11*(4), e42594. DOI: 10.1016/j.heliyon.2025.e42594.

Khetarpal, N. & Khanna, I. (2016). Dengue fever: Causes, complications, and vaccine strategies. *Journal of Immunology Research*, *2016*, 1–14. DOI: 10.1155/2016/6803098.

Kshirsagar, S. G. & Rao, R. V. (February 27, 2021). Antiviral and immunomodulation effects of Artemisia. *Medicina (Mex)*, *57*(3), 217. DOI: 10.3390/medicina57030217.

Kwissa, M., Nakaya, H. I., Onlamoon, N., Wrammert, J., Villinger, F., Perng, G. C., Yoksan, S., Pattanapanyasat, K., Chokephaibulkit, K., Ahmed, R. & Pulendran, B. (July 9, 2014). Dengue virus infection induces expansion of a CD14(+)CD16(+) monocyte population that stimulates plasmablast differentiation. *Cell Host & Microbe*, *16*(1), 115–127. PMID: 24981333. DOI: 10.1016/j.chom.2014.06.001.

Latif, M. A., Noman, M. A., Ahmmed, R., Hossain, M. S., Ahmed, M. F., Pappu, M. A. A., Islam, M. S., Noor, T., Kabir, M. H. & Mollah, M. N. H. (October 7, 2025). In-silico identification of host-key-genes associated with dengue-virus-infections highlighting their pathogenetic mechanisms and therapeutic agents. Selvaraj C, editor. *PLoS One*, *20*(10), e0333509. DOI: 10.1371/journal.pone.0333509.

Li, L., Chen, L., Wang, Y., Xie, L., Fu, S. & Wu, J. (March 2026). Discovery and characterization of a novel marafivirus from Artemisia argyi plants. *Archives of Virology*, *171*(3), 63. DOI: 10.1007/s00705-025-06492-2.

Li, J., Shi, F., Chen, D.-Q., Cao, H.-L., Xiong, B., Shen, J.-K. & He, J.-H. (2015). FS23 binds to the N-terminal domain of human Hsp90: A novel small inhibitor for Hsp90. *Nuclear Science and Techniques*, *26*, 060502. DOI: 10.13538/j.1001-8042/nst.26.060503.

Liang, Y., De Wispelaere, M., Carocci, M., Liu, Q., Wang, J., Yang, P. L. & Gray, N. S. (March 9, 2017). Structure–activity relationship study of QL47: A broad-spectrum antiviral agent. *ACS Medicinal Chemistry Letters*, *8*(3), 344–349. DOI: 10.1021/acsmedchemlett.7b00008.

Lv, J., Song, X., Luo, Z., Huang, D., Xiao, L. & Zou, K. (February 12, 2025). Luteolin: Exploring its therapeutic potential and molecular mechanisms in pulmonary diseases. *Frontiers in Pharmacology*, *16*, 1535555. DOI: 10.3389/fphar.2025.1535555.

Nascimento, E. J., Braga-Neto, U., Calzavara-Silva, C. E., Gomes, A. L., Abath, F. G. C., Brito, C. A. A., Cordeiro, M. T., Silva, A. M., Magalhães, C., Andrade, R., Gil, L. H. V. G. & Marques, E. T. A. (November 19, 2009). Gene expression profiling during early acute febrile stage of dengue infection can predict the disease outcome. *PLoS One*, *4*(11), e7892. DOI: 10.1371/journal.pone.0007892. PMID: 19936257.

Nie, C., Trimpert, J., Moon, S., Haag, R., Gilmore, K., Kaufer, B. B. & Seeberger, P. H. (December 2021). In vitro efficacy of Artemisia extracts against SARS-CoV-2. *Virology Journal*, *18*(1), 182. DOI: 10.1186/s12985-021-01651-8.

Nigam, M., Atanassova, M., Mishra, A. P., Pezzani, R., Devkota, H. P., Plygun, S., Salehi, B., Setzer, W. N. & Sharifi-Rad, J. (July 2019). Bioactive compounds and health benefits of *Artemisia* species. *Natural Product Communications*, *14*(7), 1934578X19850354. DOI: 10.1177/1934578X19850354.

NIH. (2026). AKT1 AKT serine/threonine kinase 1 [Homo sapiens (human)]. https://www.ncbi.nlm.nih.gov/gene/207.

Nofal, S. M., Mahmoud, S. S., Ramadan, A., Soliman, G. A. & Fawzy, R. (January 2009). Anti-diabetic effect of Artemisia judaica extracts. *Research Journal of Medicine and Medical Sciences*, *4*(1), 42–48.

Oliveros, J. C. (2007–2015). Venny. An interactive tool for comparing lists with Venn's diagrams. https://bioinfogp.cnb.csic.es/tools/venny/.

Otasek, D., Morris, J. H., Bouças, J., Pico, A. R. & Demchak, B. (December 2019). Cytoscape Automation: Empowering workflow-based network analysis. *Genome Biology*, *20*(1), 2498. DOI: 10.1186/s13059-019-1758-4.

Patočka, J. & Plucar, B. (July 31, 2003). Pharmacology and toxicology of absinthe. *Journal of Applied Biomedicine*, *1*(4), 199–205. DOI: 10.32725/jab.2003.036.

Pestana, C. R. & Rodrigues, G. J. (June 8, 2026). Consensus transcriptional signature of dengue virus infection reveals coordinated interferon suppression and stress-response activation. *Cell Biochemistry and Biophysics*, *366*(W1), 1423. DOI: 10.1007/s12013-026-02094-0.

Pettersen, E. F., Goddard, T. D., Huang, C. C., Couch, G. S., Greenblatt, D. M., Meng, E. C. & Ferrin, T. E. (October 2004). UCSF Chimera—a visualization system for exploratory research and analysis. *Journal of Computational Chemistry*, *25*(13), 1605–1612. DOI: 10.1002/jcc.20084.

Phadungsombat, J., Nakayama, E. E. & Shioda, T. (June 28, 2024). Unraveling dengue virus diversity in Asia: An epidemiological study through genetic sequences and phylogenetic analysis. *Viruses*, *16*(7), 1046. DOI: 10.3390/v16071046.

Ritchie, M. E., Phipson, B., Wu, D., Hu, Y., Law, C. W., Shi, W. & Smyth, G. K. (April 20, 2015). Limma powers differential expression analyses for RNA-sequencing and microarray studies. *Nucleic Acids Research*, *43*(7), e47. DOI: 10.1093/nar/gkv007.

Rogers, K. (2026). Artemisinin. Encyclopedia Britannica. https://www.britannica.com/science/artemisinin.

Salazar, MaI., Del Angel, R. M., Lanz-Mendoza, H., Ludert, J. E. & Pando-Robles, V. (December 2014). The role of cell proteins in dengue virus infection. *Journal of Proteomics*, *111*, 6–15. DOI: 10.1016/j.jprot.2014.06.002.

Schor, S. & Einav, S. (February 2018). Repurposing of kinase inhibitors as broad-spectrum antiviral drugs. *DNA and Cell Biology*, *37*(2), 63–69. DOI: 10.1089/dna.2017.4033.

Schrödinger, L., DeLano, W. (2020). PyMOL [Internet]. Available from: http://www.pymol.org/pymol.

ScienceDirect. (2015). Estrogen receptor alpha. https://www.sciencedirect.com/topics/biochemistry-genetics-and-molecular-biology/estrogen-receptor-alpha.

Screaton, G., Mongkolsapaya, J., Yacoub, S. & Roberts, C. (December 2015). New insights into the immunopathology and control of dengue virus infection. *Nature Reviews Immunology*, *15*(12), 745–759. DOI: 10.1038/nri3916.

Seema & Jain, S. K. (July 2005). Molecular mechanism of pathogenesis of dengue virus: Entry and fusion with target cell. *Indian Journal of Clinical Biochemistry*, *20*(2), 92–103. DOI: 10.1007/BF02867407.

Shaer, N., Mohamed, A. & Schnug, E. (December 17, 2025). Potential of *A. annua* bioactives as antiviral agents against SARS-CoV-2 and other health complications. *Pharmaceuticals*, *18*(12), 1904. DOI: 10.3390/ph18121904.

Sinha, S., Singh, K., Ravi Kumar, Y. S., Roy, R., Phadnis, S., Meena, V., Bhattacharyya, S. & Verma, B. (April 22, 2024). Dengue virus pathogenesis and host molecular machineries. *Journal of Biomedical Science*, *31*(1), 43. DOI: 10.1186/s12929-024-01030-9.

Sun, P., García, J., Comach, G., Vahey, M. T., Wang, Z., Forshey, B. M., Morrison, A. C., Sierra, G., Bazan, I., Rocha, C., Vilcarromero, S., Blair, P. J., Scott, T. W., Camacho, D. E., Ockenhouse, C. F., Halsey, E. S. & Kochel, T. J. (July 11, 2013). Sequential waves of gene expression in patients with clinically defined dengue illnesses reveal subtle disease phases and predict disease severity. Farrar J, editor. *PLoS Neglected Tropical Diseases*, *7*(7), e2298. DOI: 10.1371/journal.pntd.0002298.

Swamikannu, B., Umapathy, V. R., Natarajan, P. M., Nandini, M., Queency Stylin, A. G. S., Vimalarani, V. & Rajinikanth, S. (December 2024). Unlocking the therapeutic benefits of *A. annua*: A comprehensive overview of its medicinal properties. *Journal of Pharmacy and Bioallied Sciences*, *16*(Suppl 5), S4248–S4253. DOI: 10.4103/jpbs.jpbs_1250_24.

Szklarczyk, D., Kirsch, R., Koutrouli, M., Nastou, K., Mehryary, F., Hachilif, R., Gable, A. L., Fang, T., Doncheva, N T., Pyysalo, S., Bork, P., Jensen, L J. & von Mering, C. (January 6, 2023). The STRING database in 2023: Protein–protein association networks and functional enrichment analyses for any sequenced genome of interest. *Nucleic Acids Research*, *51*(D1), D638–D646. DOI: 10.1093/nar/gkac1000.

Tanenbaum, D. M., Wang, Y., Williams, S. P. & Sigler, P. B. (May 26, 1998). Crystallographic comparison of the estrogen and progesterone receptor's ligand binding domains. *Proceedings of the National Academy of Sciences*, *95*(11), 5998–6003. DOI: 10.1073/pnas.95.11.5998.

Toro-Domínguez, D., Martorell-Marugán, J., López-Dominguez, R., García-Moreno, A., González-Rumayor, V., Alarcón-Riquelme, M. E. & Carmona-Sáez, P. (2018). ImaGEO: Integrative gene expression meta-analysis from GEO database. *Bioinformatics*, *35*, bty721. DOI: 10.1093/bioinformatics/bty721.

Trott, O. & Olson, A. J. (2009). AutoDock Vina: Improving the speed and accuracy of docking with a new scoring function, efficient optimization, and multithreading. *Journal of Computational Chemistry*, *31*, 455–461. DOI: 10.1002/jcc.21334.

Tuiskunen Bäck, A. & Lundkvist, Å (January 2013). Dengue viruses—an overview. *Infection Ecology & Epidemiology*, *3*(1), 19839. DOI: 10.3402/iee.v3i0.19839.

Uno, N. & Ross, T. M. (December 2018). Dengue virus and the host innate immune response. *Emerging Microbes & Infections*, *7*(1), 1–11. DOI: 10.1038/s41426-018-0168-0.

Villordo, S. M., Filomatori, C. V., Sánchez-Vargas, I., Blair, C. D. & Gamarnik, A. V. (January 30, 2015). Dengue virus RNA structure specialization facilitates host adaptation. Nagy PD, editor. *PLOS Pathogens*, *11*(1), e1004604. DOI: 10.1371/journal.ppat.1004604.

Wan, C., Liang, Q., Ma, Y., Wang, Y., Sun, L., Lai, J., Wu, J. & Chen, Z. (March 27, 2025). Luteolin: A natural product with multiple mechanisms for atherosclerosis. *Frontiers in Pharmacology*, *16*, 1503832. DOI: 10.3389/fphar.2025.1503832.

Wu, W. I., Voegtli, W. C., Sturgis, H. L., Dizon, F. P., Vigers, G. P. A. & Brandhuber, B. J. (September 23, 2010). Crystal structure of human AKT1 with an allosteric inhibitor reveals a new mode of kinase inhibition. Gerrard JA, editor. *PLoS One*, *5*(9), e12913. DOI: 10.1371/journal.pone.0012913.

Yap, S. S. L., Nguyen-Khuong, T., Rudd, P. M. & Alonso, S. (July 25, 2017). Dengue virus glycosylation: What do we know? *Frontiers in Microbiology*, *8*, 1415. DOI: 10.3389/fmicb.2017.01415.

Zhang, Z. R., Zhang, H. Q., Li, X. D., Deng, C. L., Wang, Z., Li, J. Q., Li, N., Zhang, Q. Y., Zhang, H. L., Zhang, B. & Ye, H. Q. (October 2020). Generation and characterization of Japanese encephalitis virus expressing GFP reporter gene for high throughput drug screening. *Antiviral Research*, *182*, 104884. DOI: 10.1016/j.antiviral.2020.104884.

Zhu, Y., Chen, S., Lurong, Q. & Qi, Z. (April 23, 2023). Recent advances in antivirals for Japanese encephalitis virus. *Viruses*, *15*(5), 1033. DOI: 10.3390/v15051033.